The Electromagnetic Field of an Insulated Antenna in a Conducting or Dielectric Medium

RONOLD W. P. KING, LIFE FELLOW, IEEE, B. S. TREMBLY, MEMBER, IEEE, AND J. W. STROHBEHN, SENIOR MEMBER, IEEE

Abstract —Insulated antennas are useful for localized heating as in the hyperthermia treatment of tumors and the extraction of shale oil. The distribution of current in and the admittance of a center-driven dipole embedded in a general medium are reviewed. Formulas for the electric field generated by the currents in the dipole are derived for all points outside the antenna. Near the antenna, the field is elliptically polarized. Formulas for the polarization ellipses are derived and evaluated for antennas with electrical half-lengths $\beta_L h = \pi/4, \pi/2, \pi$, and $3\pi/2$, where $k_L = \beta_L + i\alpha_L$ is the wavenumber of the current, and this is different from the wavenumber of the ambient medium.

I. Introduction

The insulated dipole and monopole are useful not only in subsurface communication but also in localized heating. This is accomplished by the embedding of a suitably designed insulated antenna [1] into the material to be heated. One such application—which is of primary interest to the authors of this paper—is the insertion of an insulated antenna into a tumor to produce local hyperthermia in conjunction with radiation therapy [2], [3]. This application requires antennas of very small size operated at a very high frequency. A theoretically similar but practically very different use of insulated antennas for localized heating is in the extraction of shale oil. For this purpose, very large insulated antennas are inserted into boreholes in the shale and heated at an appropriate much lower frequency. In both applications, interest is primarily in the field quite close to the antenna where most of the heating takes place. The near electric field of a bare or insulated dipole in a medium like muscle or the earth is much more involved than the far field because it is elliptically polarized. Simple expressions in closed form are not available. The determination of the field of an insulated dipole is further complicated by the fact that the wavenumber for the current in the antenna is complex and different from the wavenumber of the surrounding medium.

Manuscript received January 12, 1983; revised March 3, 1983. This research was supported in part by the National Science Foundation under Grant ECS-8025818 with Dartmouth College, and in part by the Joint Services Electronics Program under Contract N00014-75-C-0648 with Harvard University.

R. W. P. King is with the Gordon McKay Laboratory, Harvard University, Cambridge, MA 02138.

B. S. Trembly and J. W. Strohbehn are with the Thayer School of Engineering, Dartmouth College, Hanover, NH 03755.

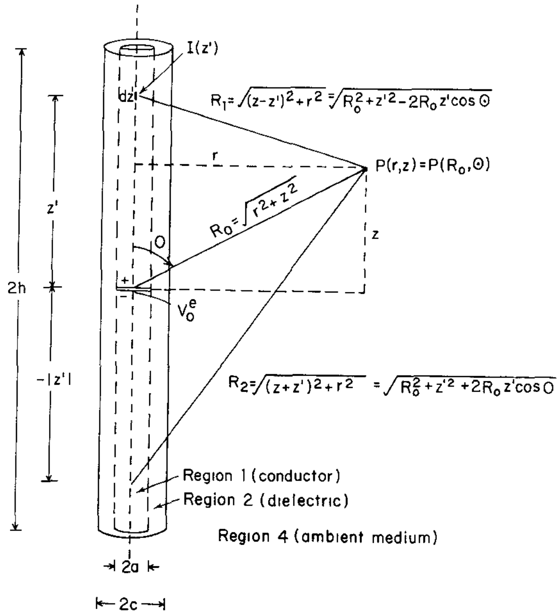

Fig. 1. Insulated dipole in ambient medium.

II. The Properties of the Insulated Dipole

An insulated dipole (Fig. 1) consists of a central conductor (Region 1) with the half-length h and radius a surrounded by a cylinder of dielectric which may consist of one or two layers (Regions 2 and 3), respectively, with the outer radii b and c. Outside this insulating sheath is the infinite ambient medium (Region 4) which may be conducting or dielectric. The central conductor is sufficiently highly conducting to be well approximated by a perfect conductor. The wavenumbers of the dielectric layers are $k_2 = \omega(\mu_0\epsilon_2)^{1/2}$ and $k_3 = \omega(\mu_0\epsilon_3)^{1/2}$, where ϵ_2 and ϵ_3 are taken to be real since the dielectrics actually used are highly nonconducting. The wavenumber of the conducting or dielectric ambient medium is $k_4 = \beta_4 + i\alpha_4 = \omega(\mu_0\tilde{\epsilon}_4)^{1/2}$, $\tilde{\epsilon}_4 = \epsilon_4 + i\sigma_4/\omega$.

The general theory of the insulated antenna applies

0018-9480/83/0700-0574$01.00

when the wavenumber of the ambient medium is large compared to that of the insulating sheath and the cross section of the antenna is electrically small. That is

$$|k_4/k_2|^2 \gg 1; \quad |k_4/k_3|^2 \gg 1; \quad (k_2 b)^2 \ll 1; \quad (k_3 c)^2 \ll 1. \tag{1}$$

Subject to these conditions and with the time dependence $e^{-i\omega t}$, the current in the central conductor is [1], [4]–[6]

$$I(z) = I(0)\frac{\sin k_L(h-|z|)}{\sin k_L h}$$

$$I(0) = V_0^e Y_0 = V_0^e / Z_0 \tag{2a}$$

where the admittance is

$$Y_0 = -(i/2Z_c)\tan k_L h. \tag{2b}$$

For a dielectric with two layers

$$k_L = k_2\left[\frac{\ln(c/a)}{\ln(b/a)+n_{23}^2\ln(c/b)}\right]^{1/2}\left[\frac{\ln(c/a)+F}{\ln(c/a)+n_{24}^2 F}\right]^{1/2} \tag{3}$$

$$Z_c = (\omega\mu_0 k_L/2\pi k_2^2)[\ln(b/a) + n_{23}^2\ln(c/b)+n_{24}^2 F] \tag{4}$$

where $n_{23}^2 = k_2^2/k_3^2$, $n_{24}^2 = k_2^2/k_4^2$, and $F = H_0^{(1)}(k_4 c)/k_4 c H_1^{(1)}(k_4 c)$. These formulas can be simplified by the introduction of an effective wavenumber k_{2e} and an effective permittivity ϵ_{2e} for an equivalent dielectric composed of a single layer with the outer radius c, viz.,

$$k_{2e} = k_2\left[\frac{\ln(c/a)}{\ln(b/a)+n_{23}^2\ln(c/b)}\right]^{1/2}$$

$$\epsilon_{2e} = \epsilon_2\left[\frac{\ln(c/a)}{\ln(b/a)+n_{23}^2\ln(c/b)}\right]. \tag{5}$$

With (5), the above formulas become

$$k_L = k_{2e}[\ln(c/a)+F]^{1/2}[\ln(c/a)+n_{24}^2 F]^{-1/2} \tag{6}$$

$$Z_c = (\omega\mu_0 k_L/2\pi k_{2e}^2)[\ln(c/a)+n_{2e4}^2 F] \tag{7}$$

where $n_{2e4}^2 = k_{2e}^2/k_4^2$. The charge per unit length associated with the current is

$$q(z) = -\frac{i}{\omega}\frac{\partial I(z)}{\partial z} = \frac{V_0^e k_L}{2\omega Z_c}\frac{\cos k_L(h-z)}{\cos k_L h}, \quad 0 \leqslant z \leqslant h \tag{8}$$

$$q(-z) = -q(z). \tag{9}$$

Since the field outside the insulator can be calculated as accurately and more simply with the equivalent single layer, this will be used. The cylindrical components of the electromagnetic field in the effective single-layer insulator, $a \leqslant r \leqslant c$, with permittivity ϵ_{2e} and wavenumber k_{2e} are approximated by

$$B_{2\phi}(r,z) \sim \frac{\mu_0 I(z)}{2\pi r} = \frac{\mu_0 I(0)}{2\pi r}\frac{\sin k_L(h-|z|)}{\sin k_L h}, \quad -h \leqslant z \leqslant h \tag{10}$$

$$E_{2r}(r,z) \sim \frac{q(z)}{2\pi\epsilon_{2e} r} = \frac{ik_L I(0)}{2\pi\epsilon_{2e} r\omega}\frac{\cos k_L(h-z)}{\sin k_L h}, \quad 0 \leqslant z \leqslant h \tag{11a}$$

$$= -\frac{ik_L I(0)}{2\pi\epsilon_{2e} r\omega}\frac{\cos k_L(h+z)}{\sin k_L h}, \quad -h \leqslant z \leqslant 0. \tag{11b}$$

A somewhat less accurate but adequate value of the small axial component of the electric field is obtained from one of Maxwell's equations by differentiation and integration. Thus

$$E_{2z}(r,z) \sim \int_a^r\left[\frac{\partial E_{2r}(r,z)}{\partial z} - i\omega B_{2\phi}(r,z)\right]dr = -\frac{i\omega\mu_0 I(0)}{2\pi}\ln(r/a)\left(1-\frac{k_L^2}{k_{2e}^2}\right)\cdot\frac{\sin k_L(h-|z|)}{\sin k_L h}. \tag{12}$$

III. The Electric Field Maintained by the Antenna

The electric field outside the antenna in Region 4 is given by [5, p. 523, eq. (7.12)]

$$\vec{E}_4(r,z) = \frac{1}{4\pi}\int_{-h}^{h} dz'\int_{-\pi}^{\pi} r'\,d\phi'\big[i\omega B_{4\phi}(c,z')\psi'(z,z')\hat{z}' - E_{4z}(c,z')\hat{\phi}'\times\nabla'\psi'(z,z') + E_{4r}(c,z')\nabla'\psi'(z,z')\big] \tag{13}$$

where

$$\psi'(z,z') = \frac{e^{ik_4 R_1'}}{R_1'}$$

$$R_1' = \left[(z-z')^2 + r^2 - 2rr'\cos\phi' + r'^2\right]_{r'=c}^{1/2} \tag{14}$$

Here R_1' is expressed in the cylindrical coordinates r, ϕ, z locating the point $P(r,z)$ where the field is calculated and r', ϕ', z' with $r' = c$ on the surface of the insulating cylinder where the source fields are defined. These last are obtained from (10)–(12) with the following boundary conditions at $r = c$:

$$B_{4\phi}(c,z') = B_{2\phi}(c,z')$$

$$E_{4r}(c,z') = (\epsilon_{2e}/\tilde{\epsilon}_4)E_{2r}(c,z')$$

$$E_{4z}(c,z') = E_{2z}(c,z'). \tag{15}$$

(Note that $\epsilon_{2e}/\tilde{\epsilon}_4 = \omega^2\mu_0\epsilon_{2e}/\omega^2\mu_0\tilde{\epsilon}_4 = k_{2e}^2/k_4^2$.) Owing to rotational symmetry, the field at $r, 0, z$ is the same as at r, ϕ, z; therefore, ϕ has been set equal to zero in (14). The operator ∇' is with respect to the primed coordinates r', ϕ', z' locating the source points. In cylindrical coordinates, $\nabla' = \hat{r}'(\partial/\partial r') + \hat{\phi}'(1/r')(\partial/\partial\phi') + \hat{z}'(\partial/\partial z')$. Note that $\nabla = \hat{r}(\partial/\partial r) + \hat{z}(\partial/\partial z)$ since $\partial/\partial\phi = 0$.

The first problem in the determination of the field given by (13) is the evaluation of the three integrals with respect to ϕ', specifically for an antenna that is sufficiently thin so that

$$|k_4 c|^2 \ll 1. \tag{16}$$

This is carried out in Appendix A. With the notation $\psi(z,z') = e^{ik_4R_1}/R_1$, $R_1 = [(z-z')^2 + r^2]^{1/2}$, where R_1 is the distance from the point of observation to the element dz', the results are

$$\int_{-\pi}^{\pi} \psi'(z,z')\, d\phi' \sim 2\pi\psi(z,z') \tag{17}$$

$$\int_{-\pi}^{\pi} \nabla'\psi'(z,z')\, d\phi' \sim -2\pi\left[\hat{r}\frac{\partial\psi(z,z')}{\partial r} + \hat{z}\frac{\partial\psi(z,z')}{\partial z}\right] \tag{18}$$

$$\int_{-\pi}^{\pi} \hat{\phi}' \times \nabla'\psi'(z,z')\, d\phi' \sim \pi c\left[\hat{r}\frac{\partial^2\psi(z,z')}{\partial z\,\partial r} - \hat{z}\frac{\partial^2\psi(z,z')}{\partial r^2}\right]. \tag{19}$$

When (10)–(12), (15), and (17)–(19) are used in (13) and the $\hat{r}$ and $\hat{z}$ components are separated, (13) becomes

$$\begin{aligned} E_{4z}(r,z) = \frac{i\omega\mu_0 I(0)}{4\pi\sin k_L h}&\left\{\int_{-h}^{h} \sin k_L(h-|z'|)\psi(z,z')\,dz'\right. \\ &- \frac{k_L}{k_4^2}\left[\int_0^h \cos k_L(h-z')\frac{\partial\psi(z,z')}{\partial z}dz'\right. \\ &\left. - \int_{-h}^{0} \cos k_L(h+z')\frac{\partial\psi(z,z')}{\partial z}dz'\right] \\ &+ \frac{1}{2}\left(\frac{k_L^2}{k_{2e}^2} - 1\right)c^2 \ln\frac{c}{a} \\ &\left.\cdot\int_{-h}^{h} \sin k_L(h-|z'|)\frac{\partial^2\psi(z,z')}{\partial r^2}dz'\right\} \end{aligned} \tag{20}$$

$$\begin{aligned} E_{4r}(r,z) = -\frac{i\omega\mu_0 I(0)}{4\pi\sin k_L h}& \\ \cdot&\left\{\frac{k_L}{k_4^2}\left[\int_0^h \cos k_L(h-z')\frac{\partial\psi(z,z')}{\partial r}dz'\right.\right. \\ &\left. - \int_{-h}^{0} \cos k_L(h+z')\frac{\partial\psi(z,z')}{\partial r}dz'\right] \\ &+ \frac{1}{2}\left(\frac{k_L^2}{k_{2e}^2} - 1\right)c^2 \ln\frac{c}{a} \\ &\left.\cdot\int_{-h}^{h} \sin k_L(h-|z'|)\frac{\partial^2\psi(z,z')}{\partial z\,\partial r}dz'\right\}. \end{aligned} \tag{21}$$

The integrals that contain $\partial/\partial z$ can be integrated by parts by setting $\partial/\partial z = -\partial/\partial z'$. This is carried out in Appendix B. The resulting formulas are

$$\begin{aligned} E_{4z}(r,z) = \frac{i\omega\mu_0 I(0)}{4\pi\sin k_L h}&\left\{\left(1 - \frac{k_L^2}{k_4^2}\right)\int_0^h \sin k_L(h-z')\right. \\ &\cdot[\psi(z,z') + \psi(z,-z')]\,dz' + \frac{k_L}{k_4^2}[\psi(z,h) \\ &+ \psi(z,-h) - 2\psi(z,0)\cos k_L h] \\ &+ \frac{1}{2}\left(\frac{k_L^2}{k_{2e}^2} - 1\right)c^2 \ln\frac{c}{a}\int_0^h \sin k_L(h-z')\frac{\partial^2}{\partial r^2} \\ &\left.\cdot[\psi(z,z') + \psi(z,-z')]\,dz'\right\} \end{aligned} \tag{22}$$

$$\begin{aligned} E_{4r}(r,z) = -\frac{i\omega\mu_0 I(0)}{4\pi\sin k_L h}&\left\{\frac{k_L r}{k_4^2}\int_0^h \cos k_L(h-z')\right. \\ &\cdot\left[\left(\frac{ik_4}{R_1} - \frac{1}{R_1^2}\right)\psi(z,z') - \left(\frac{ik_4}{R_2} - \frac{1}{R_2^2}\right)\right. \\ &\left.\cdot\psi(z,-z')\right]dz' - \frac{1}{2}\left(\frac{k_L^2}{k_{2e}^2} - 1\right)k_L c^2 \ln\frac{c}{a} \\ &\cdot\int_0^h \cos k_L(h-z')\frac{\partial}{\partial r} \\ &\left.\cdot[\psi(z,z') - \psi(z,-z')]\,dz'\right\} \end{aligned} \tag{23}$$

where, as shown in Fig. 1

$$R_1 = \left[(z-z')^2 + r^2\right]^{1/2}; \quad R_2 = \left[(z+z')^2 + r^2\right]^{1/2} \tag{24a}$$

$$\psi(z,z') = e^{ik_4R_1}/R_1; \quad \psi(z,-z') = e^{ik_4R_2}/R_2. \tag{24b}$$

Also

$$\frac{\partial^2\psi(z,z')}{\partial r^2} = \left\{\frac{ik_4}{R_1} - \frac{1}{R_1^2} - \frac{r^2}{R_1^2}\left[k_4^2 + \frac{3ik_4}{R_1} - \frac{3}{R_1^2}\right]\right\}\psi(z,z') \tag{24c}$$

$$\frac{\partial^2\psi(z,-z')}{\partial r^2} = \left\{\frac{ik_4}{R_2} - \frac{1}{R_2^2} - \frac{r^2}{R_2^2}\left[k_4^2 + \frac{3ik_4}{R_2} - \frac{3}{R_2^2}\right]\right\}\psi(z,-z'). \tag{24d}$$

With the conditions $|k_L c|^2 < |k_4 c|^2 \ll 1$, $(c/R_1)^2 \ll 1$, $(c/R_2)^2 \ll 1$, it follows that the terms $k_L c^2(\partial/\partial r)[\psi(z,z') - \psi(z,-z')]$ and $c^2(\partial^2/\partial r^2)[\psi(z,z') + \psi(z,-z')]$ are negligible, so that the final formulas for the field of a thin antenna with $|k_4 c|^2 \ll 1$ at points that satisfy $R_1^2 \gg c^2$,

$R_2^2 \gg c^2$ are

$$E_{4z}(r,z) = \frac{i\omega\mu_0 I(0)}{4\pi \sin k_L h}\left\{\left(1-\frac{k_L^2}{k_4^2}\right)\cdot\int_0^h \sin k_L(h-z')[\psi(z,z')+\psi(z,-z')]\,dz' + \frac{k_L}{k_4^2}[\psi(z,h)+\psi(z,-h) - 2\psi(z,0)\cos k_L h]\right\} \quad (25)$$

$$E_{4r}(r,z) = -\frac{i\omega\mu_0 I(0)}{4\pi \sin k_L h}\frac{k_L r}{k_4^2}\cdot\int_0^h \cos k_L(h-z')\left[\left(\frac{ik_4}{R_1}-\frac{1}{R_1^2}\right)\psi(z,z') - \left(\frac{ik_4}{R_2}-\frac{1}{R_2^2}\right)\psi(z,-z')\right]dz'. \quad (26)$$

The integrals in (25) and (26) must be evaluated numerically. Approximate values of the field nearer the antenna than permitted by the conditions $R_1^2 \gg c^2$, $R_2^2 \gg c^2$ can be obtained by interpolation between (25) and (26) and the fields on the surface $r = c$ of the antenna. These latter are given by (15) with (10)–(12). (See Appendix C.)

In the far field, defined by $R_0 = (z^2 + r^2)^{1/2} \gg h > c$, the formulas (25) and (26) can be simplified since $R_1 \sim R_0 - z'\cos\Theta$, $R_2 \sim R_0 + z'\cos\Theta$ in phases and $R_1 \sim R_2 \sim R_0$ in amplitudes, where R_0 and Θ are spherical coordinates. With these values

$$E_{4z}^r(R_0,\Theta) \sim \frac{i\omega\mu_0 I(0)}{2\pi \sin k_L h}\frac{e^{ik_4R_0}}{R_0}\left\{\left(1-\frac{k_L^2}{k_4^2}\right)\cdot\int_0^h \sin k_L(h-z')\cos(k_4 z'\cos\Theta)\,dz' + \frac{k_L}{k_4^2}[\cos(k_4 h\cos\Theta)-\cos k_L h]\right\} \quad (27)$$

$$E_{4r}^r(R_0,\Theta) \sim -\frac{i\omega\mu_0 I(0)}{2\pi \sin k_L h}\frac{e^{ik_4R_0}}{R_0}\frac{k_L}{k_4}\sin\Theta\cdot\int_0^h \cos k_L(h-z')\sin(k_4 z'\cos\Theta)\,dz'. \quad (28)$$

The integrals are now elementary and are given by

$$\int_0^h \sin k_L(h-z')\cos(k_4 z'\cos\Theta)\,dz' = \left(\frac{\sin k_L h}{k_4 \sin\Theta}\right)F_0(\Theta,k_4h,k_Lh) \quad (29)$$

and

$$\int_0^h \cos k_L(h-z')\sin(k_4 z'\cos\Theta)\,dz' = \left(\frac{\sin k_L h \cot\Theta}{k_L}\right)F_0(\Theta,k_4h,k_Lh) \quad (30)$$

where

$$F_0(\Theta,k_4h,k_Lh) = \frac{[\cos(k_4 h\cos\Theta)-\cos k_L h]\sin\Theta}{[(k_L/k_4)-(k_4/k_L)\cos^2\Theta]\sin k_L h}. \quad (31)$$

When (29) is substituted in (27) and (30) in (28), the results are

$$E_{4z}^r(R_0,\Theta) \sim \frac{i\omega\mu_0 I(0)}{2\pi k_4}\frac{e^{ik_4R_0}}{R_0}F_0(\Theta,k_4h,k_Lh)\sin\Theta \quad (32)$$

$$E_{4r}^r(R_0,\Theta) \sim -\frac{i\omega\mu_0 I(0)}{2\pi k_4}\frac{e^{ik_4R_0}}{R_0}F_0(\Theta,k_4h,k_Lh)\cos\Theta. \quad (33)$$

These cylindrical components can be combined to give the spherical components $E_\Theta^r = E_r^r\cos\Theta - E_z^r\sin\Theta$ and $E_R^r = E_r^r\sin\Theta + E_z^r\cos\Theta$. The result is

$$E_\Theta^r(R_0,\Theta) = -\frac{i\omega\mu_0 I(0)}{2\pi k_4}\frac{e^{ik_4R_0}}{R_0}F_0(\Theta,k_4h,k_Lh)$$
$$E_R^r(R_0,\Theta) = 0. \quad (34)$$

It is readily verified that when $k_L = k_4$, (22) and (23) reduce to the field of a bare conductor in Region 4 with a sinusoidally distributed current. The electric field of such an antenna is given by [7, p. 58, eqs. (11a)–(11c)] when $k_4 = \beta_0$ and by [8, p. 257, (4.2.21) and (4.2.22)] when these are corrected by the insertion of $\sin kh$ in the denominator. Also, with $k_L = k_4$, (31) reduces to the familiar far-field pattern of a bare antenna with a sinusoidally distributed current. Note, however, that $\sin k_L(h-|z|)$ is a much better approximation of the current in an insulated antenna than is $\sin k(h-|z|)$ for the bare antenna either in air with $k = \beta_0$ real or in a general medium with $k = k_4$.

IV. The Polarization of the Electric Field

Since the two mutually perpendicular components $E_{4z}(r,z)$ and $E_{4r}(r,z)$ given by (22) and (23) are not in phase, the resultant electric field in Region 4 is elliptically polarized. In order to determine the maximum value of $\vec{E}(r,z)$ and its direction, it is necessary to determine the polarization ellipses. This can be accomplished from the instantaneous values of the two components. Thus

$$\vec{E}_4(r,z,t) = \text{Real part } \vec{E}_4(r,z)e^{-i(\omega t-\theta_z)} = |E_{4z}(r,z)|[\hat{z}\cos(\omega t-\theta_z)+\hat{r}K\cos(\omega t-\theta_z+\theta_K)] \quad (35)$$

where

$$Ke^{-i\theta_K} = \frac{E_{4r}(r,z)}{E_{4z}(r,z)}; \qquad K = \left|\frac{E_{4r}(r,z)}{E_{4z}(r,z)}\right|$$

$$-\theta_K = \arg\left[\frac{E_{4r}(r,z)}{E_{4z}(r,z)}\right]; \qquad \theta_z = \arg\left[E_{4z}(r,z)\right]. \quad (36)$$

With the subscript 4 and the arguments r, z temporarily omitted for simplicity

$$E_z(t) = E_z\cos(\omega t - \theta_z) \quad (37a)$$

$$\begin{aligned} E_r(t) &= E_z K\left[\cos(\omega t - \theta_z)\cos\theta_K - \sin(\omega t - \theta_z)\sin\theta_K\right] \\ &= K\left\{E_z(t)\cos\theta_K - \left[E_z^2 - E_z^2(t)\right]^{1/2}\sin\theta_K\right\}. \end{aligned} \quad (37b)$$

The last equation can be rearranged in the standard form for an ellipse, viz.

$$Az^2 + Bzr + Cr^2 + F = 0 \quad (38)$$

with

$$A = K^2; \quad B = -2K\cos\theta_K; \quad C = 1; \quad F = -K^2E_z^2\sin^2\theta_K \quad (39)$$

where $z = E_z(t)$ and $r = E_r(t)$. In the general equation (38) of an ellipse, the term in zr can be removed by a rotation of the axes through an angle θ defined by

$$\tan 2\theta = \frac{2\tan\theta}{1-\tan^2\theta} = \frac{2K\cos\theta_K}{1-K^2}. \quad (40)$$

The angle θ is the angle of tilt of the polarization ellipse from the vertical, i.e., the angle between the major axis of the ellipse and the z axis. The equation of the ellipse referred to the new axes z' and r' is

$$A'z'^2 + C'r'^2 + F = 0 \quad (41)$$

where

$$A' = A\cos^2\theta + B\sin\theta\cos\theta + C\sin^2\theta \quad (42a)$$

$$C' = A\sin^2\theta - B\sin\theta\cos\theta + C\cos^2\theta. \quad (42b)$$

Referred to the electric vector and arranged in standard form

$$E_a^2(t)/E_a^2 + E_b^2(t)/E_b^2 = 1 \quad (43)$$

where the semi-major axis E_a and semi-minor axis E_b of the ellipse are

$$E_a = E_z(K/K')\sin\theta_K; \quad E_b = E_z(K/L')\sin\theta_K \quad (44)$$

with

$$K'^2 = K^2\cos^2\theta - 2K\cos\theta_K\sin\theta\cos\theta + \sin^2\theta \quad (45)$$

$$L'^2 = K^2\sin^2\theta + 2K\cos\theta_K\sin\theta\cos\theta + \cos^2\theta. \quad (46)$$

The ratio of major to minor axis is

$$\text{Ratio} = \frac{E_a}{E_b} = \cot\theta\left[\frac{1+2K\cos\theta_K\tan\theta + K^2\tan^2\theta}{1-2K\cos\theta_K\cot\theta + K^2\cot^2\theta}\right]^{1/2} \quad (47)$$

V. Application to a Dipole Useful in Hyperthermia

The antenna which will be used as an example in the determination of the electric field is thin enough to be inserted in a catheter embedded in a tumor. For simplicity and for general interest, the antenna will be assumed to be a center-driven dipole rather than the more complicated structure used in hyperthermia cancer therapy. The inner conductor is assigned the successive electrical half-lengths $\beta_L h = \pi/4$, $\pi/2$, π, $3\pi/2$ at $f = 915$ MHz; its radius is $a = 0.47$ mm. The antenna was constructed from Cooner CZ-1105-1 flexible gold-plated, copper-braided cable with a 33-Ω characteristic impedance. The insulating dielectric has two layers, an inner layer of air with outer radius $b = 0.584$ mm and relative permittivity $\epsilon_{2r} = 1$, and an outer layer (plastic tube) with outer radius $c = 0.80$ mm and relative permittivity $\epsilon_{3r} = 1.78$. For an equivalent single layer, $\epsilon_{2er} = 1.373$. The infinite ambient medium is given the properties of human brain tissue with the real relative permittivity $\epsilon_{4r} = 42.5$ and the real effective conductivity $\sigma_4 = 0.88$ S/m. The wavenumbers of the three materials and for the equivalent single-layer dielectric are

$$k_2 = 19.2\ \text{m}^{-1}; \quad k_3 = 25.6\ \text{m}^{-1}$$

$$k_{2e} = 22.5\ \text{m}^{-1}; \quad k_4 = 127.5 + i25.\text{m}^{-1}. \quad (48)$$

Note that with $|k_4c|^2 = 0.01$, $(k_{2e}c)^2 = 3.24\times10^{-4}$, and $|k_4/k_{2e}|^2 = 33.3$, the conditions (1) and (16) are well satisfied. The wavenumber k_L and characteristic impedance Z_c of the insulated antenna are

$$k_L = 50.6 + i10.7\ \text{m}^{-1}; \quad Z_c = 71.4 + i16.3\ \Omega. \quad (49)$$

In order to have an experimental check on the degree in which the theory approximates the properties of the actual antenna, the driving-point impedance was both calculated and measured over a wide range of lengths. In order to approximate a dipole, a monopole over a ground plane was used. The results for the monopole are shown in the complex plane in Fig. 2. A part of the difference between the theoretical and measured impedances is due to the thinness of the antenna which makes it difficult to have it perfectly straight and accurately centered in the plastic tube. Measurements with deliberately bent and eccentrically located antennas indicate that differences in reactance up to 8 or 10 Ω and resistance up to 4 or 5 Ω are possible as compared with a perfectly straight, accurately centered antenna. Further differences between theory and experiment are a consequence of the finite size of the ground plane (diameter ~ 10 cm ~ $2\lambda_4$) used in the measurements, and of junction effects [9] for which no corrections were made. When account is taken of these physical differences between the ideal conditions assumed in the theory and those obtaining in the measurements for a practical antenna for use in hyperthermia, the agreement is quite satisfactory [10].

The theoretical distributions of current along four insulated monopoles with the electrical lengths $\beta_L h = \pi/4$, $\pi/2$, π, and $3\pi/2$ are shown in Fig. 3. The electric field in

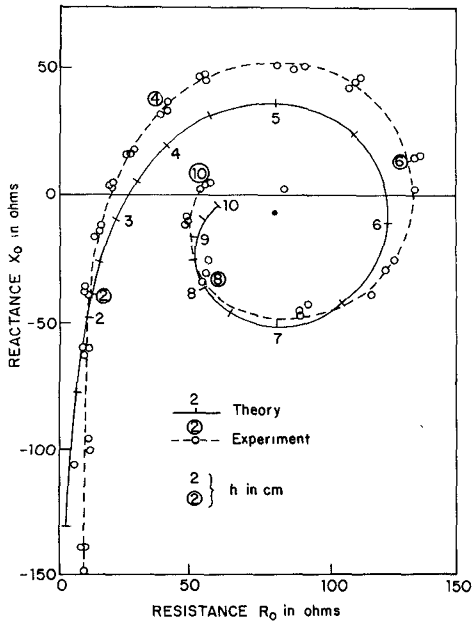

Fig. 2. Impedance $Z_0 = R_0 - iX_0$ of insulated monopole in a dissipative medium; $k_L = 50.6 + i10.7\ \mathrm{m}^{-1}$; $Z_c = 71.4 + i16.3\ \Omega$.

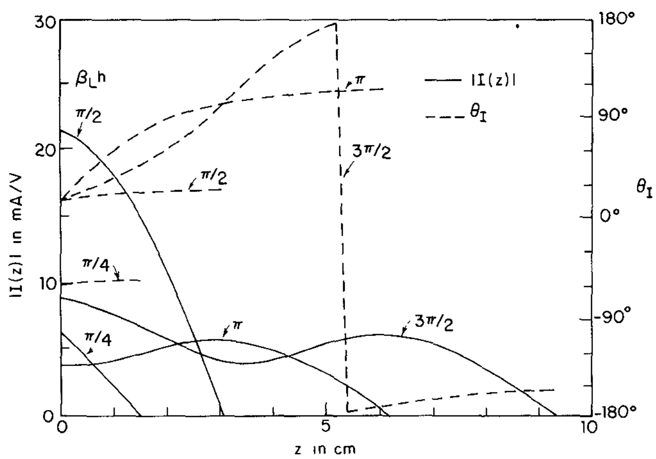

Fig. 3. Current in insulated monopole in a dissipative medium; $k_L = 50.6 + i10.7\ \mathrm{m}^{-1}$; $Z_c = 71.4 + i16.3\ \Omega$; $I(z) = |I(z)|\exp(-i\theta_I)$; $\theta_I = \tan^{-1}(I_I/I_R)$.

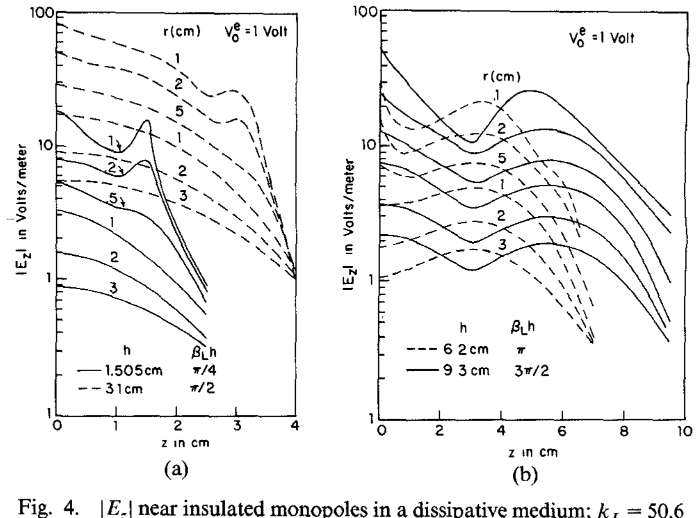

Fig. 4. $|E_z|$ near insulated monopoles in a dissipative medium; $k_L = 50.6 + i10.7\ \mathrm{m}^{-1}$; $Z_c = 71.4 + i16.3\ \Omega$. (a) $h = 1.505$ and 3.1 cm; (b) $h = 6.2$ and 9.3 cm.

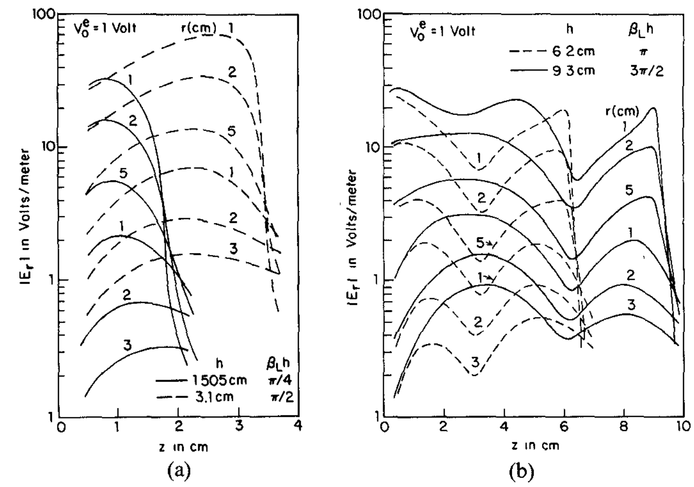

Fig. 5. $|E_r|$ near insulated monopoles in a dissipative medium; $k_L = 50.6 + i10.7\ \mathrm{m}^{-1}$; $Z_c = 71.4 + i16.3\ \Omega$. (a) $h = 1.505$ and 3.1 cm; (b) $h = 6.2$ and 9.3 cm.

a typical quadrant of the surrounding medium (Region 4) has been calculated for each of these four lengths from (25) and (26). To evaluate the two integrals in these expressions, the complex value of each integrand was computed for each of a sequence of discrete values of z'. The real and imaginary parts were then treated separately. As functions of z', they were integrated numerically by fitting cubic spline polynomials [11]. The complex values of the two definite integrals were then formed from the real and imaginary parts, and the evaluation of (25) and (26) was completed. In the evaluation, the expression (2a) was used for $I(0)$ with the driving emf $V_0^e = 1$ V. The calculated values of $|E_z|$ and $|E_r|$ are displayed graphically in Figs. 4(a) and (b) and 5(a) and (b) as functions of axial distance parallel to the antenna with the radial distance from its axis as the parameter. Close to the antenna and not too near its open end, $|E_z|$ varies roughly like $|I_z|$ and $|E_r|$ like $q(z)$. The graphs in Figs. 4(a) and (b) and 5(a) and (b) show that the electric field decreases very rapidly with increasing radial distance from the antenna. The field is, of course, rotationally symmetric about the axis of the antenna.

The radial and axial components of the electric field were combined in the manner described in Section IV to obtain the polarization ellipses shown in Figs. 6–9 for the four lengths. Each ellipse represents the path traced by the arrow end of the electric vector in one cycle when its other end is fixed at the center of the ellipse. The scale of the ellipses in these figures was adjusted to permit meaningful graphs. The actual values of the fields can be obtained from Figs. 4(a) and (b) and 5(a) and (b) which are in volts per meter for a driving emf of 1 V. The electric fields in Figs. 7–9 are superficially similar to the elliptically polarized field of a bare antenna with $\beta_4 h = \pi/2$, π and $3\pi/2$, as shown in [7, figs. 8.4, 8.6, 9.1 of ch. V], [8, p. 278], and [12, fig. 6]. However, if immersed in the same ambient

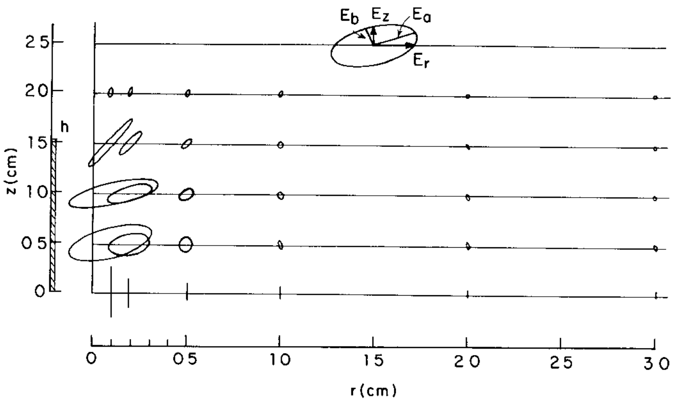

Fig. 6. Electric field of an insulated monopole with $\beta_L h \sim \pi/4$ in a dissipative medium; $h = 1.505$ cm, $k_L = 50.6 + i10.7$ m^{-1}; $Z_c = 71.4 + i16.3$ Ω.

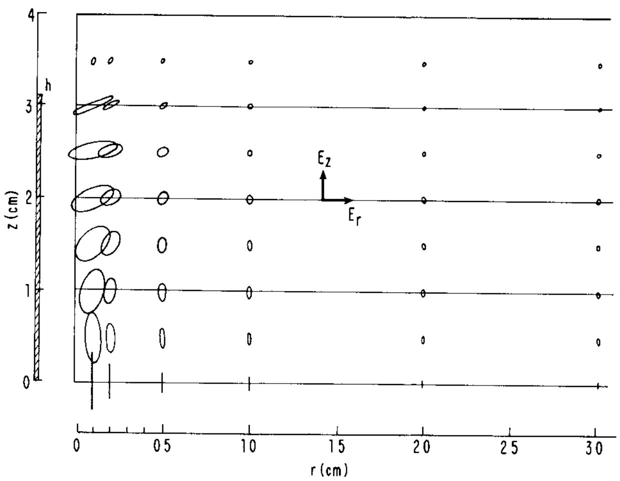

Fig. 7. Electric field of an insulated monopole with $\beta_L h \sim \pi/2$ in a dissipative medium; $h = 3.1$ cm, $k_L = 50.6 + i10.7$ m^{-1}; $Z_c = 71.4 + i16.3$ Ω.

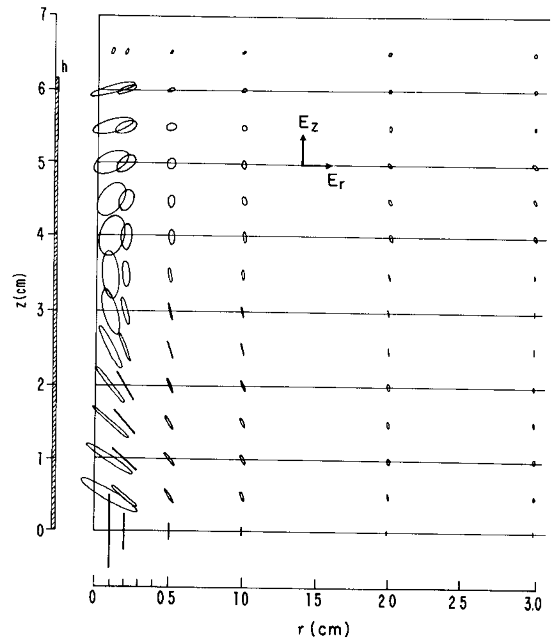

Fig. 8. Electric field of an insulated monopole with $\beta_L h \sim \pi$ in a dissipative medium; $h = 6.2$ cm, $k_L = 50.6 + i10.7$ m^{-1}; $Z_c = 71.4 + i16.3$ Ω.

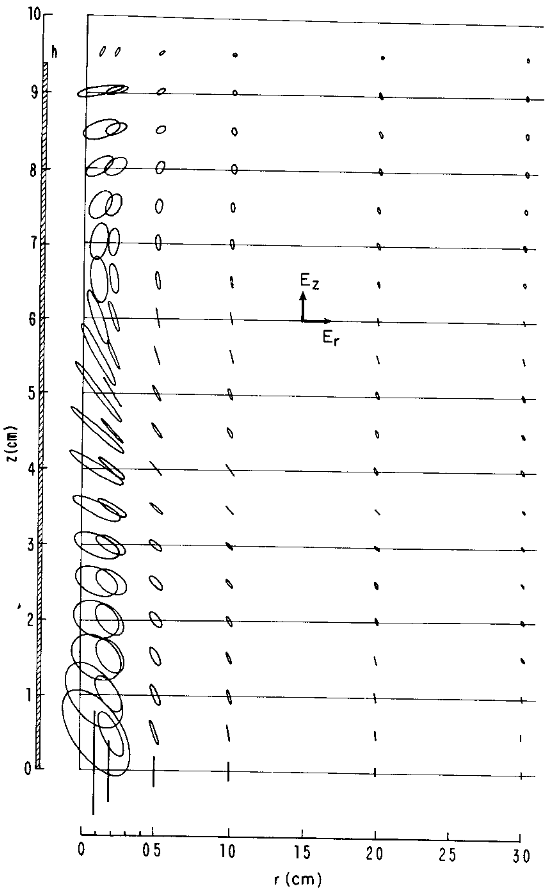

Fig. 9. Electric field of an insulated monopole with $\beta_L h \sim 3\pi/2$ in a dissipative medium; $h = 9.3$ cm, $k_L = 50.6 + i10.7$ m^{-1}; $Z_c = 71.4 + i16.3$ Ω.

medium, the actual lengths are very different since $\beta_4 = 127.5$ m^{-1}, whereas $\beta_L = 50.6$ m^{-1}. It follows that for $\beta_L h = \pi/2$, $h = 3$ cm for the insulated antenna, and for $\beta_4 h = \pi/2$, $h = 1.2$ cm for the bare antenna.

It is to be noted that if the elliptically polarized field is investigated experimentally with a small movable dipole, the measurements do not reproduce the polarization ellipses but quite different polarization patterns. This is discussed and the patterns displayed in [8, sec. 4.9], [12, pp. 282, 283].

Also of interest is the rate of heat generation as a function of location relative to the antenna. The power per unit volume of tissue dissipated in heat is given by $(1/2)\sigma_4 \vec{E} \cdot \vec{E}^* = (1/2)\sigma_4(|E_r|^2 + |E_z|^2)$, where $\sigma_4 = \sigma_{04} + \omega\epsilon_4''$ is the real effective conductivity of the ambient medium. The power dissipated per unit volume per Watt input to the antenna, i.e., $\sigma_4(|E_r|^2 + |E_z|^2)/V_0^{e2}G_0$, where G_0 is the input conductance of the antenna, has been calculated. The distribution of power dissipated as heat is shown in Fig. 10 in several planes along the lengths of the antennas with the radial distance from the antenna as the variable. Since the volume in which most of the power is dissipated is roughly proportional to the length of the antenna, the quantity actually plotted for ready comparison is $m\sigma_4(|E_r|^2 + |E_z|^2)/V_0^{e2}G_0$, where $m = 1, 2, 4$, and 6 is the approximate ratio of the length of the antenna to the

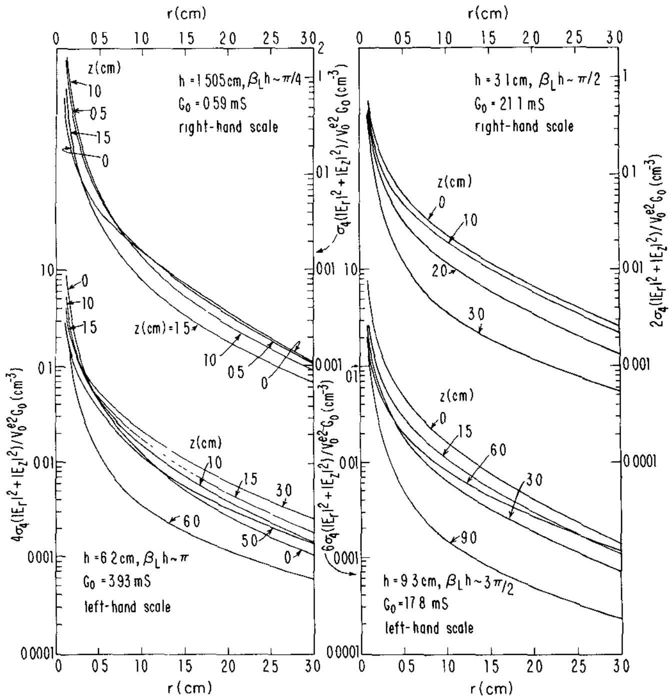

Fig. 10. Power dissipated in ambient medium in Watts/cc per input Watt to the antenna; $\sigma_4 = 0.88$ S/m, $\epsilon_{4r} = 42.5$; $k_L = 50.6 + i10.7$ m^{-1}.

length of the shortest element. The four sets of graphs indicate that the distribution of dissipated power and, hence, of heat generated is not particularly sensitive to the length of the antenna; in all cases, a cylinder surrounding the dipole absorbs comparable and fairly uniformly distributed amounts of energy over most of the length of the antenna. There is a very rapid decrease with radial distance owing to the high conductivity of the ambient medium. This emphasizes the desirability of an array of three or four insulated antennas around the volume to be heated. This configuration will be investigated in a later paper.

Appendix A

Before the integrals in (17)–(19) are evaluated, it is convenient to express the operations indicated in (18) and (19) in terms of the unprimed coordinates r, ϕ, z locating the point of observation instead of the primed coordinates r', ϕ', z' locating the source points on the surface of the antenna. This is carried out first for (18)

$$\nabla'\psi'(z,z') = \frac{\partial\psi'(z,z')}{\partial R_1'}\left[\hat{r}'\frac{\partial R_1'}{\partial r'} + \hat{\phi}'\frac{1}{r'}\frac{\partial R_1'}{\partial \phi'} + \hat{z}'\frac{\partial R_1'}{\partial z'}\right]. \tag{A1}$$

With $\partial R_1'/\partial r' = (r' - r\cos\phi')/R_1'$, $(1/r')(\partial R_1'/\partial\phi') = (r\sin\phi')/R_1'$, $\partial R_1'/\partial z' = -(z-z')/R_1'$ and, from Fig. 11, $\hat{r}' = \hat{r}\cos\phi' + \hat{\phi}\sin\phi'$, $\hat{\phi}' = -\hat{r}\sin\phi' + \hat{\phi}\cos\phi'$, $\hat{z}' = \hat{z}$, it follows that

$$\nabla'\psi'(z,z') = \left[\partial\psi'(z,z')/R_1'\partial R_1'\right] \cdot\left[\hat{r}(r'\cos\phi' - r) + \hat{\phi}(r'\sin\phi') - \hat{z}(z-z')\right] \tag{A2}$$

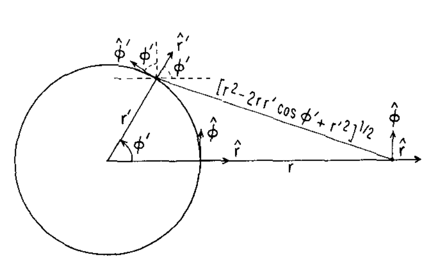

Fig. 11. Cross section of conductor with radius $r' = c$, and unit vectors $\hat{r}', \hat{\phi}'$ and $\hat{r}, \hat{\phi}$.

and

$$\int_{-\pi}^{\pi} \nabla'\psi'(z,z')\,d\phi' = 2\int_0^{\pi}\left[\partial\psi'(z,z')/R_1'\partial R_1'\right] \cdot\left[\hat{r}(r'\cos\phi' - r) - \hat{z}(z-z')\right]d\phi'. \tag{A3}$$

It is readily verified that the integrand in (A3) is simply $-\nabla\psi'(z,z')$. Hence

$$\int_{-\pi}^{\pi} \nabla'\psi'(z,z')\,d\phi' = -2\left(\hat{r}\frac{\partial}{\partial r} + \hat{z}\frac{\partial}{\partial z}\right)\int_0^{\pi}\psi'(z,z')\,d\phi'. \tag{A4}$$

The integral on the right in (A4) is the same as the integral in (17).

The integral in (19) is evaluated in a similar manner as follows:

$$\begin{aligned}\int_{-\pi}^{\pi} \hat{\phi}'\times\nabla'\psi'(z,z')\,d\phi' &= -\int_{-\pi}^{\pi}\hat{\phi}'\times\nabla\psi'(z,z')\,d\phi' \\ &= -\int_{-\pi}^{\pi}\left[(\hat{\phi}'\times\hat{r})\frac{\partial\psi'(z,z')}{\partial r} + (\hat{\phi}'\times\hat{z})\frac{\partial\psi'(z,z')}{\partial z}\right]d\phi'.\end{aligned} \tag{A5}$$

With $\hat{\phi}' = -\hat{r}\sin\phi' + \hat{\phi}\cos\phi'$, it follows that $\hat{\phi}'\times\hat{r} = -\hat{z}\cos\phi'$, $\hat{\phi}'\times\hat{z} = -\hat{\phi}\sin\phi' + \hat{r}\cos\phi'$. Hence

$$\begin{aligned}\int_{-\pi}^{\pi} \hat{\phi}'\times\nabla'\psi'(z,z')\,d\phi' &= -\int_{-\pi}^{\pi}\left[\hat{r}\frac{\partial\psi'(z,z')}{\partial z}\cos\phi' - \hat{\phi}\frac{\partial\psi'(z,z')}{\partial z}\sin\phi' - \hat{z}\frac{\partial\psi'(z,z')}{\partial r}\cos\phi'\right]d\phi' \\ &= -2\left[\hat{r}\frac{\partial}{\partial z} - \hat{z}\frac{\partial}{\partial r}\right]\int_0^{\pi}\psi'(z,z')\cos\phi'\,d\phi'.\end{aligned} \tag{A6}$$

In order to evaluate the integrals in (A4) and (A6), use is made of the following integral representation of the Bessel function:

$$\int_0^{\pi} e^{-iz\cos\phi}\cos n\phi\,d\phi = (-i)^n\pi J_n(z). \tag{A7}$$

The integrands in (A4) and (A6) are first transformed with the following approximate formula for the distance R_1' defined in (14). Use is made of the distance R_1 given in

(24a).

$$R_1' = R_1\left[1 - \frac{2rc\cos\phi'}{R_1^2} - \frac{c^2}{R_1^2}\right]^{1/2} \sim R_1 - (rc/R_1)\cos\phi'. \tag{A8}$$

The approximation requires that

$$R_1^2 \gg c^2 \quad \text{or} \quad R_1 \geqslant 4c. \tag{A9}$$

For $c = 0.8$ mm, this requires $R \geqslant 3.2$ mm. With (A8)

$$\psi'(z,z') \sim \psi(z,z')e^{-i(k_4cr/R_1)\cos\phi'}\left[1 + \frac{rc}{R_1^2}\cos\phi'\right]. \tag{A10}$$

With (A10) and (A7), it follows that

$$\int_{-\pi}^{\pi} \psi'(z,z')\,d\phi' \sim 2\pi\psi(z,z') \cdot \left[J_0(k_4cr/R_1) - i(rc/R_1^2)J_1(k_4cr/R_1)\right]. \tag{A11}$$

If the condition for a thin antenna, $|k_4c|^2 \ll 1$, is now invoked, the small-argument approximations of the Bessel functions may be used. Furthermore, $(rc/R_1^2)J_1(k_4cr/R_1) \sim k_4c^2r^2/2R_1^3 \ll 1$, so that for use in (17) and (18) with (A4)

$$\int_{-\pi}^{\pi} \psi'(z,z')\,d\phi' \sim 2\pi\psi(z,z'). \tag{A12}$$

Alternatively, for use in the far zone, where in amplitudes $R_1 \sim R_0$, $r/R_0 = \sin\Theta$, and with no restriction on k_4c

$$\int_{-\pi}^{\pi} \psi'(z,z')\,d\phi' \sim 2\pi\psi(z,z')J_0(k_4c\sin\Theta). \tag{A13}$$

The evaluation of (A6) proceeds in a similar manner. With (A10) and (A7), and the relation $\cos^2\phi' = (1/2)(1+\cos 2\phi')$, it follows that

$$\int_{-\pi}^{\pi} \hat{\phi}'\times\nabla'\psi'(z,z')\,d\phi' \sim 2\pi\left[\hat{r}\frac{\partial}{\partial z} - \hat{z}\frac{\partial}{\partial r}\right] \cdot\left\{\psi(z,z')\left[iJ_1(k_4cr/R_1) - (rc/2R_1^2)J_0(k_4cr/R_1) + (rc/2R_1^2)J_2(k_4cr/R_1)\right]\right\}. \tag{A14}$$

With the small-argument approximations permitted by $|k_4c|^2 \ll 1$ and the condition $c^2/R_1^2 \ll 1$, the contribution by the term with $J_2(k_4cr/R_1)$ as a factor is negligible. Hence

$$\int_{-\pi}^{\pi} \hat{\phi}'\times\nabla'\psi'(z,z')\,d\phi' \sim \pi c\left[\hat{r}\frac{\partial}{\partial z} - \hat{z}\frac{\partial}{\partial r}\right] \cdot\left[r\left(\frac{ik_4}{R_1} - \frac{1}{R_1^2}\right)\psi(z,z')\right]. \tag{A15}$$

However, $r\left(\frac{ik_4}{R_1} - \frac{1}{R_1^2}\right)\psi(z,z') = \partial\psi(z,z')/\partial r$, so that

$$\int_{-\pi}^{\pi} \hat{\phi}'\times\nabla'\psi'(z,z')\,d\phi' = \pi c\left[\hat{r}\frac{\partial}{\partial z} - \hat{z}\frac{\partial}{\partial r}\right]\frac{\partial\psi(z,z')}{\partial r}. \tag{A16}$$

In the far zone with $r/R_1 \sim r/R_0 = \sin\Theta$

$$\int_{-\pi}^{\pi} \hat{\phi}'\times\nabla'\psi'(z,z')\,d\phi' \sim 2\pi iJ_1(k_4c\sin\Theta) \cdot\left[\hat{r}\frac{\partial}{\partial z} - \hat{z}\frac{\partial}{\partial r}\right]\psi(z,z'). \tag{A17}$$

Appendix B

The following integrals in (20) and (21) are readily transformed with integration by parts to obtain:

$$\int_{-h}^{h} \sin k_L(h-|z'|)\frac{\partial^2\psi(z,z')}{\partial z\,\partial r}dz' = -k_L\int_0^h \cos k_L(h-z')\frac{\partial}{\partial r}\left[\psi(z,z') - \psi(z,-z')\right]dz' \tag{B1}$$

$$\int_0^h \cos k_L(h-z')\frac{\partial\psi(z,z')}{\partial z}dz' - \int_{-h}^{0} \cos k_L(h+z')\frac{\partial\psi(z,z')}{\partial z}dz' = -\left[\psi(z,h) + \psi(z,-h) - 2\psi(z,0)\cos k_Lh\right] + k_L\int_0^h \sin k_L(h-z')\left[\psi(z,z') + \psi(z,-z')\right]dz'. \tag{B2}$$

Note also that

$$\frac{\partial\psi(z,z')}{\partial r} = \left(\frac{ik_4}{R_1} - \frac{1}{R_1^2}\right)r\psi(z,z') \tag{B3}$$

$$\frac{\partial\psi(z,-z')}{\partial r} = \left(\frac{ik_4}{R_2} - \frac{1}{R_2^2}\right)r\psi(z,-z'). \tag{B4}$$

Appendix C

In order to determine the electric field between the surface $r = c$ of the insulator and radial distances $r > c$ that satisfy the inequalities $R_1^2 \gg c^2$, $R_2^2 \gg c^2$ which permit the neglecting of the last terms in (22) and (23), it is possible to interpolate between the two sets of formulas. For $E_{4r}(r,z)$ this is straightforward since it decreases continuously essentially as $1/r$ outward from the surface $r = c$ of the insulator. For $E_{4z}(r,z)$ the interpolation is complicated by the fact that $E_{2z}(r,z)$ increases logarithmically from zero at $r = a$ to $r = c$ and then reaches a maximum just beyond $r = c$ in Region 4. This behavior is illustrated in Fig. 12 for a resonant monopole ($\beta_Lh = \pi/2$) at three cross sections. $|E_z(r,z)|$ is calculated from (12) for $a \leqslant r \leqslant c$ ($0.47 \leqslant r \leqslant 0.8$ mm) and from (25) for $r \geqslant 1$ mm. Similar graphs in Fig. 13 show $|E_z(r,0)|$ for monopoles with five different lengths as a function of r from $a \leqslant r \leqslant c$ ($0.7 \leqslant r \leqslant 1.0$ mm), as calculated from (12), and for $r > 1$ mm, as calculated from (25). Since the conditions $R_1^2 \gg c^2$ and $R_2^2 \gg c^2$ range from $r^2 \gg c^2$ to $(r^2 + h^2) \gg c^2$ in the range of integration, it is difficult to assess the importance of the neglected term when r is near c. Calculated points are shown in Figs. 12 and 13 with c/r as large as 0.8. Graphs constructed with

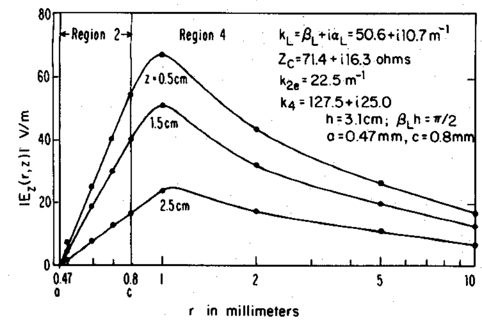

Fig. 12. Magnitude of $E_z(r, z)$ in insulator and ambient medium for resonant monopole ($\beta_L h = \pi/2$) at different cross sections z.

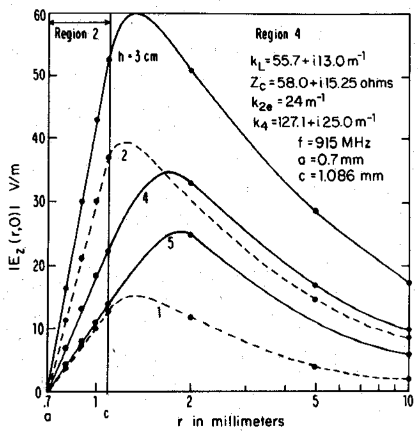

Fig. 13. Magnitude of $E_z(r,0)$ in insulator and ambient medium for monopoles of different lengths h.

them are reasonable, but they may be somewhat in error near their maxima in the range between $r = c$ and values that satisfy $r^2 \gg c^2$.

References

[1] R. W. P. King, L. C. Shen, and T. T. Wu, "Embedded insulated antennas for communication and heating," *Electromagnetics*, vol. 1, pp. 51–72, 1981.

[2] J. W. Strohbehn, E. D. Bowers, J. E. Walsh, and E. B. Douple, "An invasive microwave antenna for locally-induced hyperthermia for cancer therapy," *J. Microwave Power*, vol. 14, pp. 339–350, 1979.

[3] D. C. deSieyes, E. B. Douple, J. W. Strohbehn, and B. S. Trembly, "Some aspects of optimization of an invasive microwave antenna for local hyperthermia treatment of cancer," *Med. Phys.*, vol. 8, pp. 174–183, Mar.–Apr. 1981.

[4] R. W. P. King, K.-M. Lee, S. R. Mishra, and G. S. Smith, "Insulated linear antenna: Theory and experiment," *J. Appl. Phys.*, vol. 45, pp. 1688–1697, Apr. 1974.

[5] R. W. P. King and G. S. Smith, *Antennas in Matter*. Cambridge, MA: M.I.T. Press, 1981, Ch. 1; also, p. 510, eqs. (4.21) and (4.22).

[6] K.-M. Lee, T. T. Wu, and R. W. P. King, "Theory of an insulated antenna in a dissipative medium," *Radio Sci.*, vol. 12, pp. 195–203, Mar.–Apr. 1977.

[7] R. W. P. King, *Theory of Linear Antennas*. Cambridge, MA: Harvard University Press, 1956.

[8] R. W. P. King and C. W. Harrison, Jr., *Antennas and Waves*. Cambridge, MA: M.I.T. Press, 1969.

[9] R. W. P. King, S. R. Mishra, K.-M. Lee, and G. S. Smith, "The insulated monopole: Admittance and junction effects," *IEEE Trans. Antennas Propagat.*, vol. AP-23, pp. 172–177, 1975.

[10] B. S. Trembly, J. W. Strohbehn, and R. W. P. King, "Practical embedded insulated antenna for hyperthermia," in *Proc. 10th Annual Northeast Bio-engrg. Conf.*, Dartmouth College, Hanover, NH, March 15–16, 1982, pp. 105–108.

[11] R. W. Hornbeck, *Numerical Methods*. New York, NY: Quantum Publishers, 1975.

[12] R. W. P. King and K. Iizuka, "Field of a half-wave dipole in a dissipative medium," *IEEE Trans. Antennas Propagat.*, vol. AP-11, 275–285, May 1963.

Ronold W. P. King (A'30–SM'43–F'53) was born in Williamstown, MA, on September 19, 1905. He received the B.A. and M.S. degrees in physics from the University of Rochester, Rochester, NY, in 1927 and 1929, respectively, and the Ph.D. degree from the University of Wisconsin, Madison, in 1932, after having done graduate work at the University of Munich, Germany, and Cornell University, Ithaca, N.Y.

He served as a Teaching and Research Assistant at the University of Wisconsin from 1932 to 1934, and as an Instructor and Assistant Professor of Physics at Lafayette College, Easton, PA, from 1934 to 1937. During the academic year 1937–1938 he was a Guggenheim Fellow in Germany. In 1938 he joined the faculty of Harvard University, Cambridge, MA, where he advanced to the rank of Professor in 1946. He was a Gordon McKay Professor of Applied Physics at Harvard University until 1972, when he became Professor Emeritus. In 1958 he was again a Guggenheim Fellow.

Dr. King is a fellow of the American Physical Society and the American Academy of Arts and Sciences, and a member of the American Association of University Professors, the American Association of the Advancement of Science, Commission B of the International Union of Radio Science, Phi Beta Kappa, and Sigma Xi.

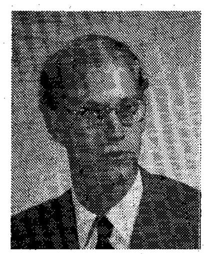

B. Stuart Trembly received the B.S. degree from Yale University, New Haven, CT, in 1975, and the Ph.D. degree from Dartmouth College, Hanover, NH, in 1982. He joined the faculty at the Thayer School of Engineering at Dartmouth College in 1982, where he is Assistant Professor.

His research interest is the application of electrical engineering to biomedical problems.

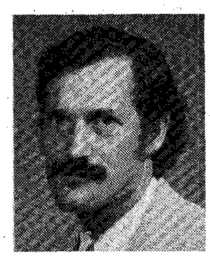

John W. Strohbehn (S'57–M'64) received the B.S., M.S., and Ph.D. degrees in electrical engineering from Stanford University, Stanford, CA, in 1958, 1959, and 1964, respectively.

He joined the faculty at the Thayer School of Engineering, Dartmouth College, Hanover, NH, in 1963, where he presently holds a position as Professor of Engineering. His research efforts have been in the fields of radiophysics, including microwave and optical propagation through the atmosphere, and in biomedical engineering, including image processing, tomography, and the use of heat in the cure and control of cancer.

Dr. Strohbehn is a Fellow of the Optical Society of America, a member of the American Association for the Advancement of Science and URSI Commission II. He was a National Academy Exchange Scientist to the Soviet Union in 1964, an Associate Editor of the IEEE Transactions on Antennas and Propagation from 1969 to 1971, and is presently Associate Editor of the IEEE Transactions on Biomedical Engineering. He was a Visiting Research Scientist at Stanford University Medical School in 1981–1982.